Composites: Part B 44 (2013) 613–619

Contents lists available at SciVerse ScienceDirect

Composites: Part B

journal homepage: www.elsevier.com/locate/compositesb

Characterization and mechanical performance comparison of multiwalled carbon nanotube/polyurethane composites fabricated by electrospinning and solution casting

Leonard D. Tijing [a,*,1], Chan-Hee Park [b,1], Woo Lim Choi [a], Michael Tom G. Ruelo [a], Altangerel Amarjargal [b,c], Hem Raj Pant [b,d], Ik-Tae Im [a], Cheol Sang Kim [a,b,*]

[a] Division of Mechanical Design Engineering, Chonbuk National University, Jeonju, Jeonbuk 561-756, Republic of Korea
[b] Department of Bionanosystem Engineering, Graduate School, Chonbuk National University, Jeonju, Jeonbuk 561-756, Republic of Korea
[c] Power Engineering School, Mongolian University of Science and Technology, Ulaanbaatar, Mongolia
[d] Department of Engineering Science and Humanities, Institute of Engineering, Pulchowk Campus, Tribhuvan University, Kathmandu, Nepal

ARTICLE INFO

Article history:
Received 7 December 2011
Received in revised form 18 January 2012
Accepted 13 February 2012
Available online 25 February 2012

Keywords:
A. Fibers
A. Polymer–matrix composites (PMCs)
A. Thin films
B. Mechanical properties
Carbon nanotubes

ABSTRACT

Multiwalled carbon nanotube/polyurethane (MWNT/PU) composites were prepared by electrospinning and solution casting. The morphological and thermal properties, and mechanical performance of the nanofiber and film composites were characterized and compared. The tensile strength of neat PU film was 9-fold higher than that of neat PU nanofibrous mat. The incorporation of MWNTs increased the tensile strength and modulus of the composite nanofibers by 69% and 140%, respectively, and 62% and 78%, respectively for composite films. The MWNT/PU composites showed an improved thermal degradation behavior, with the incorporation of low MWNT content in the composites.

1. Introduction

Polymer-based composite hybrid materials have attracted significant interests in the fields of material science and engineering. Composite materials formed by polymer/inorganic materials are attractive for the purpose of creating new materials with new or enhanced properties compared with their pristine, individual material. The hybrid material can improve the performance of the mechanical, thermal, optical, electrical, antimicrobial, biological, antifouling and catalytic properties of a polymer matrix [1,2]. Among the hybrid materials, polymer composites containing carbon nanotubes (CNTs) have been extensively studied by different groups since the report by Iijima [3]. CNTs exhibit excellent properties like high aspect ratio, very low density, small size, and excellent thermal, mechanical and electrical properties [4]. Thus, CNTs are perfect candidates as filler materials to improve the overall properties of polymer composites [5]. In order to improve the physiochemical properties of PU, CNTs (having different functionalities) are incorporated into the PU matrix to add functionalities to the composite material [6]. For improvement in mechanical and thermal properties, effective load transfer from the polymer matrix to the CNTs is needed [4,7]. Homogeneous dispersion of CNTs and strong interfacial interactions between CNTs and polymer are important requirements to enable effective load transfer. Acid-treatment of CNTs is usually carried out to modify the surface of CNTs and attach functional groups to help in the dispersion of CNTs in solvent solution and to improve the interaction of CNTs to polymer [8].

Among the polymers, polyurethane (PU) is one of the most versatile materials and is widely used in different applications [9]. There are many ways to fabricate CNT/PU composites such as solution casting, melt mixing, sol–gel method, and electrospinning [10]. Solution casting is one of the simplest fabrication methods for surface coating or making thin films [11]. Jung et al. [11] fabricated a transparent PU film incorporated with multiwalled carbon nanotubes (MWNTs) functionalized by vacuum ultraviolet (UV) light treatment by solution casting. They reported a 2-fold and 10-fold increase in tensile strength and modulus, respectively for MWNT/PU composite film as compared to neat PU film. Amr et al. [6] reported an increase of 22% in the Young's modulus of CNT/polystyrene (PS) nanocomposites, but a decrease in glass transition temperature, compared to neat PS. In recent years,

* Corresponding authors. Address: Division of Mechanical Design Engineering, Chonbuk National University, Jeonju, Jeonbuk 561-756, Republic of Korea. Tel.: +82 63 270 4284; fax: +82 63 270 2460.
E-mail addresses: ltijing@jbnu.ac.kr (L.D. Tijing), chskim@jbnu.ac.kr (C.S. Kim).
[1] These authors contributed equally to this work.

1359-8368/$ - see front matter © 2012 Elsevier Ltd. All rights reserved.
doi:10.1016/j.compositesb.2012.02.015

electrospinning has gained ground in the effective way of fabricating fibers in sub-micron scale, with high porosity and high surface-area-to-volume ratio (~1–100 m^2/g), and it has found many applications in tissue engineering, filtration, textiles and nanocomposites [12]. Jeong and his colleagues [13] reported an increase of 15% in tensile strength of MWNT/polyvinyl alcohol (PVA) nanofibers at 1 wt.% MWNT but the tensile strength was found to decrease with the increase in MWNT content. Pedicini and Farris [14] compared the mechanical properties of bulk PU film to the electrospun PU mat. They obtained the tensile properties of both bulk PU film and electrospun PU mat, and characterized the latter using SEM, and infrared dichroism. They found a difference in stress–strain behavior between the nanofibrous mat and bulk film, and concluded that this difference was due to molecular orientation within the material, and strain-induced orientation.

To the authors' knowledge, no one has compared yet the morphological, mechanical, and thermal properties of electrospun PU nanofibrous mat and solution-casted PU film when MWNTs are incorporated in the PU matrix. Both electrospinning and solution-casting are simple methods that show promise in the large-scale fabrication of MWNT/polymer composites for engineering applications, so that we used both methods in this study. Though both composite materials can be prepared from the same solution with different fabricating methods, the resulting physical, mechanical and thermal characteristics of the hybrid material are different. Thus, in the present study, we present a comparison of the mechanical and thermal properties of neat PU and MWNT/PU composite materials fabricated by electrospinning and solution-casting, and their morphologies and structures were characterized and compared.

2. Experimental details

2.1. Materials

Multi-walled carbon nanotubes (MWNTs) (diameter = 5–10 nm, length = 10–30 μm, purity > 95%) were provided by Nanosolutions, Inc. from Jeonju City, South Korea. The surfaces of the MWNTs were modified by attaching carboxylic acid functional groups through acid-treatment (HSO_4/HNO_3, 3:1, v/v%) [9]. High molecular weight thermoplastic polyurethane pellets (PU) (Estane Skythane X595A-11) were purchased from Lubrizol Advanced Materials, Inc., Cleveland, USA. The PU pellets were dried in an oven at 80 °C for at least 3 h before dissolution in solvents. Nitric acid (70% HNO_3, extra pure), sulfuric acid (98% H_2SO_4, extra pure), N, N dimethylformamide (DMF) and methyl ethyl ketone (MEK, extra pure) were bought from Showa Chemicals, Inc., Japan, and were used as received.

2.2. Fabrication of nanofibers and film

The neat PU solution was prepared by dissolving pre-dried PU pellets (10 wt.%) in DMF/MEK (50:50, wt/wt.%) by magnetic stirring. The MWNTs were dispersed in DMF/MEK by bath sonication for 3 h, replacing the distilled water in the bath sonicator every 30 min. The sonicated MWNT solution was added to the neat PU solution and was magnetically stirred for 20–24 h. The final weight of MWNTs with respect to the weight of PU in the dried composite nanofibrous mat and film was 0.1 wt.%.

The electrospinning system (Fig. 1a) was composed mainly of a high-voltage power supply, a syringe with a blunt metal needle, a syringe pump, and a grounded flat collector, all of which were placed in a sealed chamber. The needle had an inner diameter of 0.51 mm and was oriented perpendicularly to the collector, which was 150 mm away from the blunt needle tip. Electrospinning was

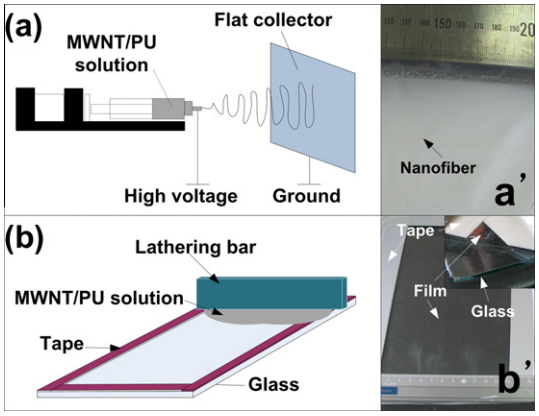

Fig. 1. Schematic of the electrospinning system (a) and solution-casting method (b) and photographic images of the electrospun nanofiber (a′) and solution-casted film (b′).

carried out at 11 kV with a feed rate of 1 ml h^{-1}. Four ml of the prepared neat PU or MWNT/PU solution was electrospun onto the flat collector at room temperature and at a relative humidity of 20–30%. In solution-casting (Fig. 1b), the set-up was composed of a glass substrate, adhesive tapes, and solid metal bar. The neat PU or MWNT/PU solution was poured slowly onto the glass substrate with adhesive tapes forming a rectangular mold, and lathered manually by a metal bar to form a uniform film. The adhesive tapes were used to control the thickness of the film. Solution casting was carried out at ambient conditions. The electrospun nanofibrous mat and solution-casted film were both dried in an oven at 80 °C for 48 h to remove the residual solvents.

2.3. Characterization and measurements

Tensile tests were performed using an Instron bench-type tensile test machine (LR5K Plus) with a load limit of 100 N according to ASTM D882-10. The crosshead speed was 5 mm/min. At least five dog-bone-shaped specimens for each sample were tested, and the average of which was used as the tensile property of the sample.

The surface and cross-section morphology and structure of the fabricated nanofibers and films were investigated by field emission scanning electron microscopy (FESEM, Hitachi S-4800, Japan) and transmission electron microscopy (TEM, H-7650, Hitachi, Japan). The samples for FESEM were coated with platinum using a Pt coater (K575x, Emitech) and examined at an accelerating voltage of 15 kV. The TEM samples for nanofibers were prepared by electrospinning directly on a copper grid mesh coated with carbon and formar for 15 s.

The distribution of fiber sizes was determined using an image processing software (ImageJ, NIH, USA), checking the diameters of at least 100 fibers and the average was calculated. The porosity measurements of the nanofibers were obtained by following the procedure of He et al. [15], using a bulk PU density of 1.2 g/cm^3. The thickness of the samples was measured by a high-precision digital microcaliper (Mitutuyo Absolute, Japan).

Water contact angle measurements were carried out using GBX, Digidrop (France) water contact angle meter. Deionized water with a drop diameter of 6 μm was automatically dropped onto the mat. The solution conductivity and viscosity were measured by a portable electrical conductivity meter (CM 40G Ver 1.09, DKK TOA Co., Japan) and by a programmable rheometer (DV III, Brookfield Co., USA), respectively.

Raman spectra of the neat and MWNT/PU composites were recorded using a Raman confocal spectroscopy (Nanofinder 30,

Japan) using a He–Ne light source at 632.8-nm with a spectral resolution of 1 cm^{-1}. The FTIR spectra of the samples were measured using a Paragon 1000 Spectrometer (Perkin Elmer, USA) in the range of 400–4000 cm^{-1} with a signal resolution of 1 cm^{-1} and a minimum of 16 scans. Thermogravimetric analysis (TGA, TA Instruments, USA) was carried out to check for the thermal stability of the samples at a heating rate of 10 °C/min from 30 to 600 °C. Differential scanning calorimetry (DSC, TA Instruments, USA) was performed at a rate of 10 °C/min in the temperature range of 30–200 °C under nitrogen atmosphere. Both TGA and DSC were performed in the same atmosphere.

3. Results and discussion

For ease of discussion, the following name conventions are used: Nmat, Cmat, Nfilm, and Cfilm referring to neat PU nanofibrous mat, MWNT/PU nanofibrous composite mat, neat PU film, and MWNT/PU composite film, respectively. The morphologies of the electrospun nanofibrous mat and solution-casted film are shown in Fig. 2. By visual observation, the nanofibrous mats appeared to be a white-colored film-like structure (see Fig. 1a′), but through FESEM observation, the electrospun nanofibrous mats (Fig. 2a and b) were actually highly-porous in structure, and had randomly-oriented, ultrafine, interlocking nanofibers. Nmat (Fig. 2a) showed fiber diameter in the range of 100–600 nm with an average of 210 ± 120 nm, while Cmat had diameters in the range of 100–950 nm with average of 340 ± 210 nm. The incorporation of MWNTs resulted in bigger fiber diameters, primarily due to the increased conductivity and viscosity (Fig. 3) of the electrospinning solution as reported in other studies [16,17]. The increased conductivity of the MWNT/PU solution also resulted in less bead formation for Cmat as compared to Nmat. Meanwhile, the solution-casted film showed solid, non-porous, smooth and transparent (Figs. 1b′ and 2d–f) film for both neat PU and MWNT/PU films. Nfilm (Fig. 2d) showed solid film with smooth and clean surface, while Cfilm also showed smooth surface but with dispersed white

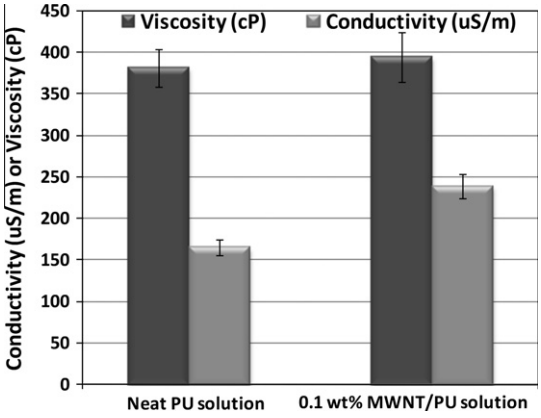

Fig. 3. Conductivity and viscosity of neat PU and 0.1 wt.% MWNT/PU solutions.

spots (see arrows in Fig. 2e, and inset), which were the protruding ends of MWNTs embedded in the film. In Fig. 2c, we can observe that the electrospun nanofibrous mat was highly porous, with a porosity of about 78%, while the composite film was solid throughout (Fig. 2e). Both nanofibrous mat and film showed a thickness of around 30 ± 5 μm. Based from these figures, we can say that for the same size and thickness of sample, the nanofibrous mat has much lower density than the solid film, but the nanofibrous mat presents much higher surface area to volume ratio, which is why electrospun nanofibers have been used in many applications such as in filtration and tissue engineering. The apparent density of Nmat was 0.3 g/cm^3, which was roughly 1/5 of the density of the bulk Nfilm (i.e., 1.2 g/cm^3). The transparency of both nanofibrous mat and film structures in the representative visible light region (~550 nm) is shown in Table 1. It shows that the film structure was generally more transparent than the nanofibrous mat structure for both neat PU and MWNT/PU composites. Especially, Nfilm exhibited excellent transparency, while Nmat appeared to be white (Fig. 1a′)

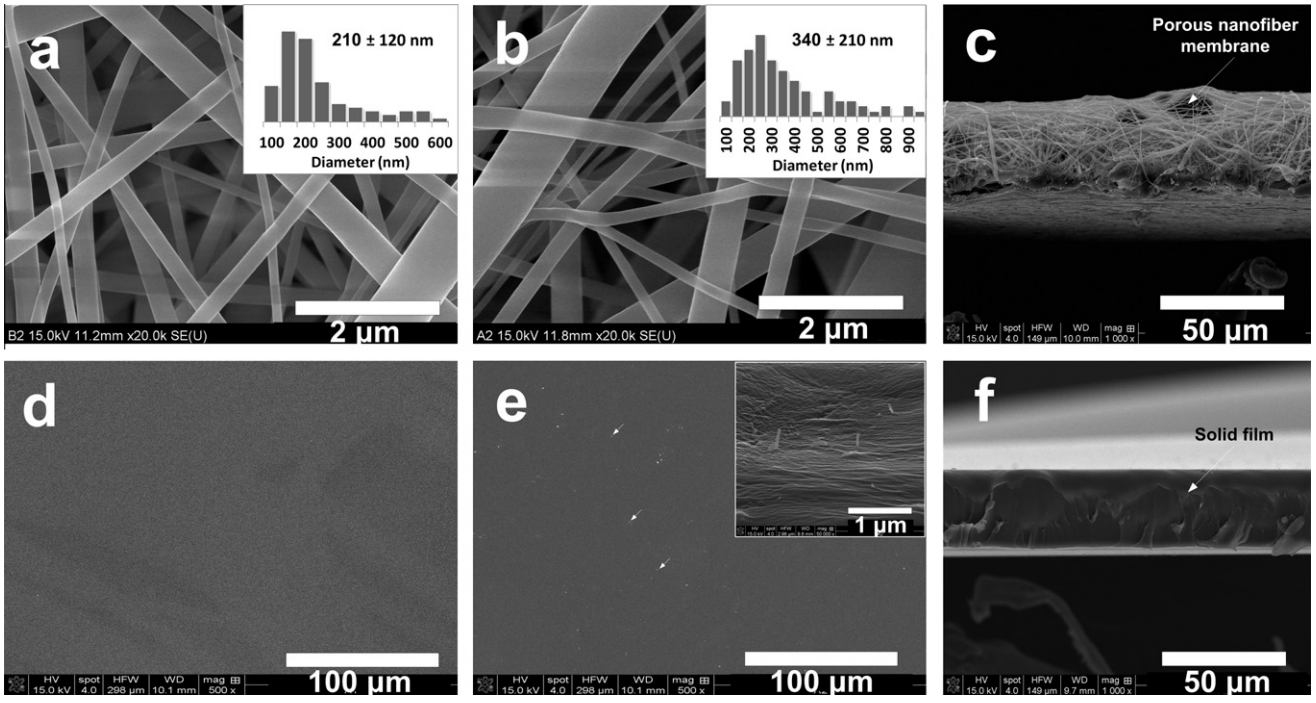

Fig. 2. FESEM images of electrospun nanofibers: (a) neat PU; (b) 0.1 wt.% MWNT/PU; (c) cross-section of (a); and solution-casted films: (d) neat PU; (e) 0.1 wt.% MWNT/PU, and (f) cross-section of (d).

Table 1
Summary of the physical and mechanical properties of the neat PU and 0.1 wt.% MWNT/PU composites.

Property/sample	Nanofiber		Film	
	Neat PU	MWNT/PU	Neat PU	MWNT/PU
Name convention	Nmat	Cmat	Nfilm	Cfilm
Fiber diameter (nm)	210 ± 120	340 ± 210	–	–
Porosity (%)	78.4	66.4	–	–
Transparency at 550 nm (%)	80.5	71.5	95.3	77.5
Tensile strength (MPa)	5.1 ± 0.2	8.6 ± 0.4	47.3 ± 4	76.6 ± 8.4
Elongation at break (%)	540 ± 105	453 ± 68	775 ± 56	960 ± 71
Modulus (MPa)	1.5 ± 0.1	3.6 ± 0.5	18.3 ± 7	32.5 ± 6.2

due to light scattering [18]. The incorporation of MWNTs reduced the transparency of both composite film and nanofibrous mat.

To check the presence of MWNTs in the composite materials, TEM imaging was carried out. The TEM image of Cmat (Fig. 4a) shows MWNTs embedded, well-encapsulated and oriented along the axis of the nanofiber, due to the high electrostatic charge during electrospinning, as well as to the high shear and elongation from whipping instability [16]. On the other hand, the MWNTs inside the film were seen to be dispersed individually in the PU matrix (Fig. 4b), appearing curved and curly, which shows the MWNTs' high flexibility. The curved structure of MWNTs in the PU matrix is reported to have lower reinforcing capacity than straight MWNTs [7].

The contact angle (CA) measurements of neat PU and MWNT/PU composites are shown in the insets of Fig. 5. Contact angle is a quantitative measure of the wettability of a surface [19]. CA varies according to the surface energy and the solid surface roughness [20]. Nmat (Fig. 5b) showed a much hydrophobic surface at CA = 125.2° compared to CA = 71.7° of Nfilm (Fig. 5c). Our present results are in good agreement with the study of Lin et al. [21], who also observed higher CAs for poly[(alanino ethyl ester)$_{0.67}$ (glycino ethyl ester)$_{0.33}$ phosphazene] (PAGP) nanofibrous mat (119°) when compared to CAs of PAGP solution-casted film (84.4°). Nmat owes its high CA to its increased surface roughness as compared to Nfilm surface. Though no surface roughness measurements were carried out in the present study, a report of Shang et al. [20] revealed a much higher surface roughness of electrospun nanofibrous mat (~300–500 nm) compared to dip-coated sol–gel films (~0.5 nm). The increase in surface roughness results in less contact area for solid and water, due to the presence of more air bubbles trapped at the interface, which leads to increased water contact angles [20]. Meanwhile, Cmat (Fig. 5a) showed a very small decrease in CA (124.8°) when compared to Nmat, which could be attributed to the increase in fiber diameters of Nmat. For solution-casted film, Cfilm (Fig. 5d) showed an increased CA (98.1°) compared to Nfilm.

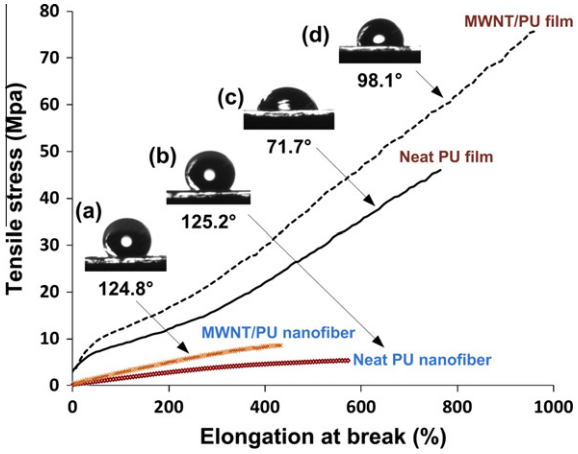

Fig. 5. Typical stress–strain behavior of neat PU and MWNT/PU composite electrospun nanofiber and solution casted film. The insets show the water contact angle measurements.

The reason for the differences in CA could be justified by checking the morphologies of the respective composites. As we can see in Fig. 4a, the MWNTs were wholly-covered and well-encapsulated by the PU matrix inside the nanofiber, thereby only exposing a pure PU surface, so that the CA of Cmat is basically similar with Nmat. On the other hand, the increased CA of Cfilm could be attributed to the presence of some protruding MWNTs at the surface (inset of Fig. 2e), which increases the surface roughness. The hydrophobic nature of protruding MWNTs could have also contributed to the increased CA. Several studies [19,22,23] have shown that the protrusion of nanofillers such as CNTs from the polymer matrix increases the surface area, wherein only the hills of the rough surface is wetted, and not the valleys, thus contributing to increased CA.

The stress–strain curves of neat PU and MWNT/PU nanofibrous mat and film are shown in Fig. 5 and Table 1. Nmat exhibited a tensile strength of 5.1 ± 0.2 MPa and an elongation of 540%. Its stress–strain curve was quite monotonic in nature showing a falling rate curve until failure. On the other hand, Nfilm showed a nonlinear behavior from 0% to 300% strain and at higher strains, a more linear curve. Nfilm had a tensile strength of 47.3 MPa, elongation of 453% and a modulus of 18.3 MPa. Comparing the two, Nfilm exhibited 9-fold higher tensile strength than Nmat. Moreover, Nfilm had also much higher modulus and elongation at break. The difference in their mechanical performance could be explained by their morphologies in Fig. 2. The low density of the nanofibrous mat, with many pores, could have affected its mechanical properties. During tensile test, the fibers which were oriented to the principal strain

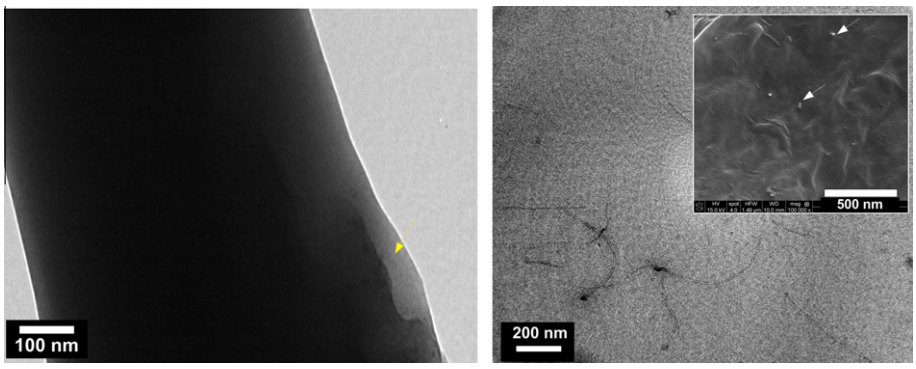

Fig. 4. (a) TEM image of a single electrospun 0.1 wt.% MWNT/PU nanofiber and (b) TEM and FESEM (inset) of solution-casted film.

direction were stretched uniaxially, while those fibers oriented in other direction experienced rotation, aligning themselves to the strain direction [24]. This phenomenon explains the low stress at the low strain region for Nmat. For Nfilm, the obtained film was solid and mechanically isotropic throughout, thus it showed a characteristic curve of an elastomeric material, i.e., a sigmoidal curve (Fig. 5). When MWNTs were incorporated into the PU matrix (Fig. 5), Cmat showed an increase in tensile strength, from 5.1 to 8.6 MPa, or an increase of 69%. The modulus also showed a more than 2-fold increase from 1.5 to 3.6 MPa, but its flexibility slightly decreased from 540% to 453%. Meanwhile, Cfilm showed similar curve pattern as with the Nfilm, but it exhibited higher mechanical properties. The tensile strength, elongation, and modulus increased by 62%, 24%, and 78%, respectively, compared to those of Nfilm. For effective load transfer of PU matrix to the MWNTs, there should be high interfacial stress between the MWNTs and PU [13,25,26]. The orientation of the MWNTs and the aspect ratio are also important factors in the effective load transfer. Generally, MWNTs in straight shape, and homogeneously dispersed in the host polymer provides better load transfer than curly-shaped MWNTs and agglomerated. In the present study, the MWNTs were homogeneously dispersed in the PU film, showing individual MWNTs enveloped by PU matrix, but were curly in shape. On the other hand, the MWNTs in the nanofiber were generally aligned along the axis of the nanofiber, especially along the surface of the nanofiber, but there was a non-uniform distribution of MWNTs in the nanofiber. This could explain the lower elongation of Cmat compared to Nmat. Furthermore, there could possibly be some agglomerations of the MWNTs in the nanofiber, which could act as stress-concentration points leading to failure [25]. The increase in tensile strength for both MWNT/PU film and nanofibrous mat could be due to the following: (a) after acid treatment of MWNTs, some form of defects was made on the surface of the MWNTs. These defects could act as anchoring sites for PU to lock in, and; (b) the acid-treatment attached some carboxylic acid groups, which could enhance the interaction of MWNTs to the OH groups of PU chain [11,27].

To help explain the enhanced mechanical properties of the composite materials, FTIR and Raman spectral analyses were carried out. Fig. 6 shows the infrared spectra of the neat PU and MWNT/PU composites. The neat PU and MWNT/PU film and nanofibrous mat composites all showed similar peaks. From Fig. 6, N–H stretching at 3290 cm^{-1}, and CH_2 stretching at 2930 cm^{-1}, reflecting the C–H asymmetrical flexing vibration [28] were observed; and the peaks at 1715 and 1700 cm^{-1}, and at 1210 cm^{-1} and 1060 cm^{-1} are assigned to C–O stretching vibrations [9], and C–O stretching, respectively. There were no big differences in the major bands, but there were differences in peak intensities for each sample showing higher intensities when MWNTs were incorporated into the PU matrix for both film and nanofibrous mat composites [16]. The area under these absorption peaks increased with the increase in MWNT content signifying the physical adhesion due to hydrogen bond between the amide group and C–O group of the PU matrix and the carboxylic group of the MWNTs [29]. The presence and interaction of MWNTs to PU are further verified by Raman spectroscopy. Fig. 7 shows the Raman spectra of the electrospun nanofibrous mat and film. Very weak peaks could be observed for both neat PU materials in the range of 1300–1700 cm^{-1}, while the MWNT/PU composites showed higher and additional intensity peaks in the same range. The peak at 1610 cm^{-1} (G-band) is designated to the ordered lattice or in-plane vibrations of the MWNTs, while the peak at 1420 cm^{-1} (D-band) is designated to the defect-induced region of the MWNTs [30,31]. These additional peaks clearly show the successful incorporation of MWNTs in the composite nanofiber and film and the increased intensities of the MWNT/PU composite materials signify good interfacial interaction of MWNTs and PU matrix, which improves the overall properties of the composite material.

The thermal stability of MWNT/PU composite film and nanofibrous mat were found to have improved as compared to their neat PU counterparts (Fig. 8). It should be noted that the present MWNT content was only 0.1 wt.%. A much better improvement in thermal stability of the composites could be possible by incorporating higher quantities of MWNT [32]. This increase could be attributed to the excellent thermal stability of the MWNTs, which were enveloped wholly by the PU matrix. The acid-treatment of MWNTs, which attached functional groups on the surface of the MWNTs, also helped in the good interaction between MWNTs and PU as verified by Raman and FTIR results. Furthermore, the differential scanning calorimetry measurements in Fig. 9 shows some shifting of the endothermic peaks of the MWNT/PU composite films and nanofibrous mat especially at 170–180 °C, which is associated with the melting of the hard segment of PU [11]. This suggests some interactions of the hard segment to MWCNTs by means of a newly-formed hydrogen bonding, which stabilizes the dynamical thermal properties of the composite films.

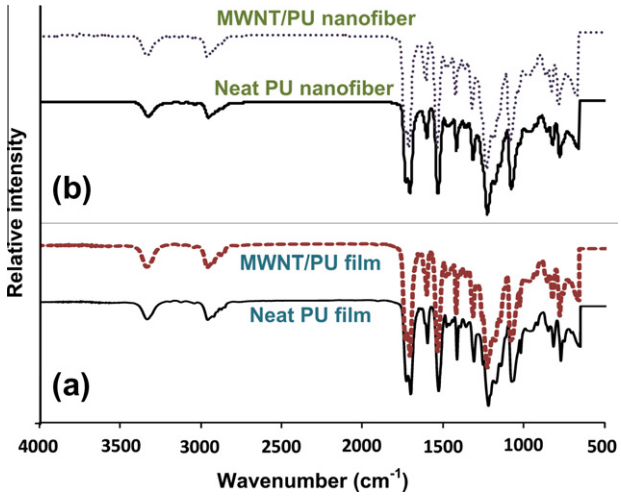

Fig. 6. FTIR spectra of neat PU and MWNT/PU composites: (a) solution-casted film and (b) electrospun nanofibers.

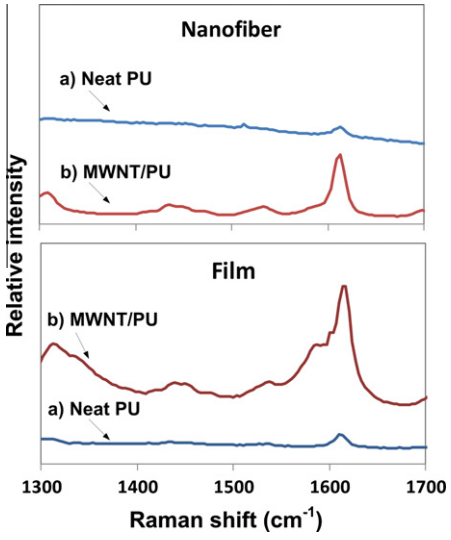

Fig. 7. Raman spectra of neat PU and MWNT/PU composite (a) film and (b) nanofibers.

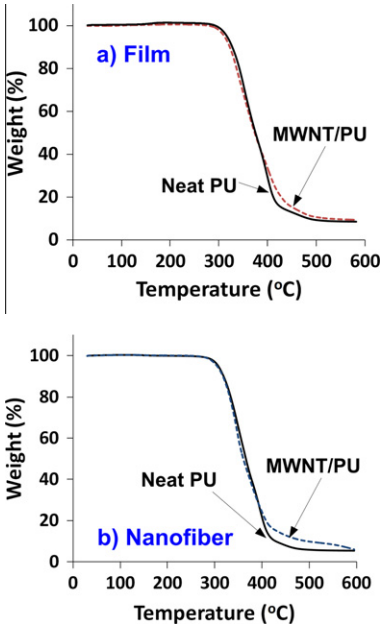

Fig. 8. Thermogravimetric analysis curves of neat PU and MWNT/PU composite (a) film and (b) nanofibers.

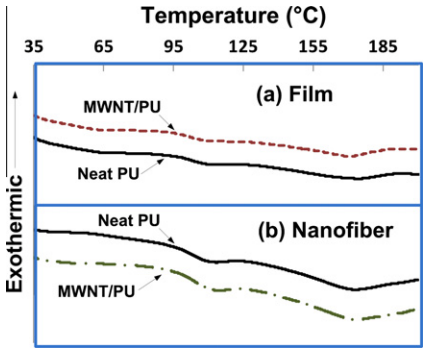

Fig. 9. Differential scanning calorimetry measurements of neat PU and MWNT/PU composite (a) film and (b) nanofibers.

4. Conclusions

We have fabricated neat PU and MWNT/PU composites by electrospinning and solution casting, and their morphological, thermal and mechanical properties were compared. Both electrospinning and solution-casting are simple methods that show promise in the large-scale fabrication of MWNT/polymer composites. The results showed that electrospun nanofibrous mats were highly porous and had a density equivalent to about 1/4–1/3 of the bulk density of PU. The neat PU film was transparent and solid, and it showed 9-fold higher tensile strength than the neat PU nanofibrous mat. The PU nanofibrous mat showed more hydrophobic surface compared to PU film due to the increase in surface roughness. Moreover, the neat PU film had also much higher modulus and elongation at break than neat PU nanofibrous mat. The incorporation of low content of MWNTs in the PU matrix has improved the overall mechanical and thermal properties of composite film and nanofibrous mat. Additional improvement could be achieved with the incorporation of higher amounts of MWNTs in the PU matrix, as long as the MWNTs are properly functionalized, and homogeneous dispersion in the polymer matrix is ensured to have effective load transfer. Electrospinning presents an easy way of aligning MWNTs along the axis of the fibers, but care must be taken for possible agglomeration of MWNTs in the nanofiber that could lead to premature failure of the composite material.

Acknowledgments

This research was supported by a Grant from the Korean Ministry of Education, Science and Technology through the National Research Foundation (Water Treatment Project No. 2011-0011807) and partially by a Grant from the Business for International Cooperative Research and Development between Industry, Academy and Research Institute funded by the Korean Small and Medium Business Administration (Project No. 00042172-1).

References

[1] Huang ZM, Zhang YZ, Ramakrishna S, Lim CT. Electrospinning and mechanical characterization of gelatin nanofibers. Polymer 2004;45:5361–8.
[2] Sarkar S, Zou J, Liu J, Xu C, An L, Zhai L. Polymer-derived ceramic composite fibers with aligned pristine multiwalled carbon nanotubes. ACS Appl Mater Interf 2010;2:1150–6.
[3] Iijima S. Helical microtubules of graphitic carbon. Nature 1991;354:56–8.
[4] Agnihotri P, Basu S, Kar KK. Effect of carbon nanotube length and density on the properties of carbon nanotube-coated carbon fiber/polyester composites. Carbon 2011;49:3098–106.
[5] Salmoria GV, Paggi RA, Lago A, Beal VE. Microstructural and mechanical characterization of PA12/MWNTs nanocomposite manufactured by selective laser sintering. Polym Test 2011;30:611–5.
[6] Amr IT, Al-Amer A, Thomas SP, Al-Harthi M, Girei SA, Sougrat R, et al. Effect of acid treated carbon nanotubes on mechanical, rheological and thermal properties of polystyrene nanocomposites. Composites Part B 2011;42:1554–61.
[7] Liu T, Phang IY, Shen L, Chow SY, Xhang WD. Morphology and mechanical properties of multiwalled carbon nanotubes reinforced nylon-6 composites. Macromolecules 2004;37:7214–22.
[8] Kwon J, Kim H. Comparison of the properties of waterborne polyurethane/multiwalled carbon nanotube and acid-treated multiwalled carbon nanotube composites prepared by in situ polymerization. J Polym Sci A: Polym Chem 2005;43:3973–85.
[9] Xia H, Song M. Preparation and characterization of polyurethane–carbon nanotube composites. Softw Matter 2005;1:386–94.
[10] Xiong J, Zheng Z, Qin X, Li M, Li H, Wang X. The thermal and mechanical properties of a polyurethane/multi-walled carbon nanotube composite. Carbon 2006;44:2701–7.
[11] Jung YC, Kim HH, Kim YA, Kim JH, Cho JW, Endo M, et al. Optically active multiwalled carbon nanotubes for transparent, conductive memory-shape polyurethane film. Macromolecules 2010;43:6106–12.
[12] Demir MM. Investigation on glassy skin formation of porous polystyrene fibers electrospun from DMF. Exp Polym Lett 2010;4:2–8.
[13] Jeong JS, Moon JS, Jeon SY, Park JH, Alegaonkar PS, Yoo JB. Mechanical properties of electrospun PVA/MWNTs composite nanofibers. Thin Solid Films 2007;515:5136–41.
[14] Pedicini A, Farris RJ. Mechanical behavior of electrospun polyurethane. Polymer 2003;44:6857–62.
[15] He W, Yong T, Teo WE, Ma Z, Ramakrishna S. Fabrication and endothelialization of collagen-blended biodegradable polymer nanofibers: potential vascular graft for blood vessel tissue engineering. Tissue Eng 2005;11:1574–88.
[16] Lu P, Hsieh YL. Multiwalled carbon nanotube (MWNT) reinforced cellulose fibers by electrospinning. ACS Appl Mater Interf 2010;2:2413–20.
[17] Ayutsede J, Gandhi M, Sukigara S, Ye H, Hsu CM, Gogotsi Y, et al. Carbon nanotube reinforced Bombyx mori silk nanofibers by the electrospinning process. Biomacromolecules 2006;7:208–14.
[18] Chen D, Wang R, Tiju WW, Liu T. High performance polyimide composite films prepared by homogeneity reinforcement of electrospun nanofibers. Compos Sci Technol 2011;71:1556–62.
[19] Roach P, Shirtcliffe NJ, Newton MI. Progress in superhydrophobic surface development. Softw Matter 2008;4:224–40.
[20] Shang HM, Wang Y, Takahashi K, Cao GZ. Nanostructured superhydrophic surfaces. J Mater Sci 2005;40:3587–91.
[21] Lin YJ, Cai Q, Fang Q, Xue LW, Jin RG, Yang XP. Effect of solvent on surface wettability of electrospun polyphosphazene nanofibers. J Appl Polym Sci 2010;115:3393–400.
[22] Choi BG, Park HS. Superhydrophobic graphene/nafion nanohybrid films with hierarchical roughness. J Phys Chem 20, in press, doi: 10.1021/jp207818b.
[23] Pavese M, Musso S, Bianco S, Giorcelli M, Pugno N. An analysis of carbon nanotube structure wettability before and after oxidation treatment. J Phys-Condens Mater 2008;20:1–7.
[24] Xu M, Zhang T, Gu B, Wu J, Chen Q. Synthesis and properties of novel polyurethane – urea/multiwalled carbon nanotube composites. Macromolecules 2006;39:3540–5.
[25] Chen W, Tao X, Liu Y. Carbon nanotube-reinforced polyurethane composite fibers. Compos Sci Technol 2006;66:3029–34.

[26] Kuan HC, Ma CM, Chang WP, Yuen SM, Wu HH, Lee TM. Synthesis, thermal, mechanical and rheological properties of multiwall carbon nanotube/waterborne polyurethane nanocomposite. Compos Sci Technol 2005;65:1703–10.
[27] Ki HS, Yeum JH, Choe SJ, Kim JH, Cheong IW. Fabrication of transparent conductive carbon nanotubes/polyurethane-urea composite films by solvent evaporation-induced self-assembly (EISA). Compos Sci Technol 2009;69:645–50.
[28] Han XJ, Huang ZM, He CL, Liu L, Wu QS. Coaxial electrospinning of PC (shell)/PU(core) composite nanofibers for textile application. Polym Compos 2006;27:381–7.
[29] Bhattarai N, Edmondson D, Veiseh O, Matsen FA, Zhang M. Electrospun chitosan-based nanofibers and their cellular compatibility. Biomaterials 2005;26(31):6176–84.
[30] Moonoosawmy KR, Kruse P. Ambiguity in the characterization of chemically modified single-walled carbon nanotubes: a Raman and ultraviolet-visible-near infrared study. J Phys Chem C 2009;113:5133–40.
[31] Dresselhaus MS, Eklund PC. Phonons in carbon nanotubes. Adv Phys 2006;49:705–814.
[32] Baji A, Mai YW, Wong SC, Abtahi M, Du X. Mechanical behavior of self-assembled carbon nanotube reinforced nylon 6, 6 fibers. Compos Sci Technol 2010;70:1401–9.